A bacterial cysteine protease effector protein interferes with photosynthesis to suppress plant innate immune responses

José J. Rodríguez-Herva, Pablo González-Melendi, Raquel Cuartas-Lanza, María Antúnez-Lamas, Isabel Río-Alvarez, Ziduo Li, Gema López-Torrejón, Isabel Díaz, Juan C. del Pozo, Suma Chakravarthy, Alan Collmer, Pablo Rodríguez-Palenzuela and Emilia López-Solanilla

Summary

The bacterial pathogen *Pseudomonas syringae* pv *tomato* DC3000 suppresses plant innate immunity with effector proteins injected by a type III secretion system (T3SS). The cysteine protease effector HopN1, which reduces the ability of DC3000 to elicit programmed cell death in non-host tobacco, was found to also suppress the production of defence-associated reactive oxygen species (ROS) and callose when delivered by *Pseudomonas fluorescens* heterologously expressing a *P. syringae* T3SS. Purified His_6-tagged HopN1 was used to identify tomato PsbQ, a member of the oxygen evolving complex of photosystem II (PSII), as an interacting protein. HopN1 localized to chloroplasts and both degraded PsbQ and inhibited PSII activity in chloroplast preparations, whereas a $HopN1_{D299A}$ non-catalytic mutant lost these abilities. Gene silencing of *NtPsbQ* in tobacco compromised ROS production and programmed cell death by DC3000. Our data reveal PsbQ as a contributor to plant immunity responses and a target for pathogen suppression.

Introduction

Effectors delivered by the type III secretion system (T3SS) are one of the main weapons of *Pseudomonas syringae* and other bacterial plant pathogens (Cunnac *et al.*, 2009). In recent years, research on these proteins has highlighted their critical function in manipulating the plant immune system (Gohre and Robatzek, 2008). Plant immunity can be classified into two forms, PAMP-triggered immunity (PTI) and effector-triggered immunity (ETI) (Chisholm *et al.*, 2006; Jones and Dangl, 2006). PTI encompasses all plant responses elicited upon challenge with pathogen/microbe-associated molecular patterns (PAMP/MAMP), whereas ETI is activated by host R proteins upon recognition of a cognate microbial effector. Although there are differences in the signals involved in initiating these processes, a common defence response is developed albeit with differences in kinetic and quantitative aspects (Boller and Felix, 2009).

Effectors can interfere with each step of plant immunity, for example, by inhibiting PAMP receptor activation, by downregulating MAPK (mitogen-activated protein kinase) signalling, by degradation of cell defence components or by modification of the defence transcriptome (Gohre and Robatzek, 2008). Therefore, effectors may target PTI, ETI or both as there is an overlap between the two types of immunity (Boller and Felix, 2009; Tsuda and Katagiri, 2010). Furthermore, a given effector could affect both responses, as exemplified by the *P. syringae* effector AvrPtoB, which suppresses both PTI and ETI (Lin *et al.*, 2006; de Torres *et al.*, 2006).

From the plant's perspective, production of reactive oxygen species (ROS) is one of the earliest cellular responses following pathogen recognition (Doke, 1983). It has been proposed that ROS can directly cause strengthening of the host cell wall (Bradley *et al.*, 1992; Huckelhoven, 2007) and contribute important signals mediating defence gene activation (Levine *et al.*, 1994). NADPH oxidase appears to be the predominant enzymatic activity

responsible for the oxidative burst in *Arabidopsis* (Torres and Dangl, 2005), although there is a growing controversy on the origin of ROS. The oxidative burst is associated with other defence-related cellular responses, particularly the hypersensitive response (HR) and the underlying induction of programmed cell death (PCD) (Mur *et al.*, 2008). The HR is a localized response at the site of pathogen attack that is associated with the limitation of pathogen spread. It has been largely studied in the context of the ETI response, and is associated with the recognition of effector proteins or their activity by the ETI surveillance system.

Hemibiotrophic pathogens like *P. syringae*, evade or suppress ETI PCD, but late in the infection process they elicit the cell death underlying disease lesions, presumably to promote pathogen dissemination. Screening for effectors that can suppress PCD has been carried out in tobacco and *Arabidopsis* (Jamir *et al.*, 2004; Guo *et al.*, 2009). The events that lead to PCD or to the death associated with disease share common steps and the main differences between both processes may reside in the number of inducing cells and the timing of the response (Lamb *et al.*, 1992; Tao *et al.*, 2003; del Pozo *et al.*, 2004). The biochemical activities of effectors that suppress PCD are just beginning to be studied and a better understanding of the targets of these proteins is likely to reveal much about the regulation of this pivotal process in the interaction of plants with hemibiotrophic pathogens (Abramovitch and Martin, 2004; Greenberg and Yao, 2004).

HopN1 is an effector protein produced by *P. syringae* pv *tomato* DC3000 (*PsPto*) that has cysteine protease activity. HopN1 suppresses cell death associated with HR in non-host tobacco plants and with disease in host tomato plants (López-Solanilla *et al.*, 2004). HopN1 possesses a catalytic triad (C172, H283, D299) that is shared with other members of the YopT/AvrPphB effector family (Shao *et al.*, 2002). HopN1 catalytic core mutants do not suppress plant cell death suggesting that HopN1 cysteine protease activity is essential for its effector function (López-Solanilla *et al.*, 2004). In addition, it has been reported that HopN1, among several other effectors, suppresses the microRNA pathway in *Arabidopsis* (Navarro *et al.*, 2008). Here, we studied HopN1 in the context of multiple immunity-associated processes and identified a novel interactor, PsbQ. Through the identification of the HopN1 target we have discovered a role for photosystem II (PSII) in pathogen-elicited plant cell death.

Results

HopN1 suppresses physiological processes associated with plant immunity

As HopN1 is able to suppress cell death, we hypothesized that it may also be capable of suppressing other related innate immune responses such as ROS production and callose deposition. We tested this in the two host plants of strain DC3000, *Arabidopsis* and tomato, through the expression of *hopN1* in *Pseudomonas fluorescens* 55 (Pf55) (pLN18), which expresses heterologously a *P. syringae* T3SS, thus enabling the delivery into plant cells of effector proteins, such as HopN1, in a manner and levels that mimic natural infections (Jamir *et al.*, 2004; López-Solanilla *et al.*, 2004; Oh *et al.*, 2010). PAMPs displayed by Pf55 generate a PTI response in inoculated plants, which is increased by the pLN18-encoded T3SS, as indicated by a higher level of ROS than that observed with Pf55 without a T3SS (Oh *et al.*, 2010). Figure 1 shows that HopN1 inhibits ROS production and callose deposition in *Arabidopsis* plants, whereas a HopN1$_{D299A}$ non-catalytic mutant version of the protein almost completely losses the inhibitory activity (see Table S1). The same pattern of inhibitory activity was observed in tomato plants (see Fig. S1). The inhibition of ROS production elicited by Pf55(pLN18) is consistent with the cell death suppression phenotype described for HopN1 during the interaction of DC3000 with its hosts, because ROS production is known to be involved in PCD.

HopN1 targets photosystem II

With the aim of identifying plant targets of HopN1 we developed an *in vitro* pull-down assay using as bait the immobilized HopN1 protein and as a prey a tomato leaf extract. After the resolution of eluates by liquid chromatography, we detected five differential peaks (see Fig. S2A). Mass spectrometric (MS) analysis identified one of the differential peaks, peak #3, as the tomato protein PsbQ, which is one of the members of the oxygen evolving complex (OEC) of photosystem II (PSII) (see Fig. S2B). This protein is involved in the stabilization of the complex that catalyses the photolysis of water, the first step in the non-cyclic electron transport of photosynthesis (Roose *et al.*, 2007). During this process, two molecules of water are oxidized to one molecule of oxygen and four protons, with the generation of four electrons that travel through the photosynthetic electron transport chain.

To confirm that the binding observed with tomato leaf samples was not a result of indirect interactions we developed an *in vitro* pull-down assay using MalE-PsbQ purified protein as the prey and HopN1-His$_6$ as the bait. Using antibodies against both the PsbQ or the MalE-tag, we could observe that PsbQ is retained specifically by the HopN1 immobilized protein while we were not able to detect any binding of the HopN1$_{D299A}$ mutant to PsbQ (Fig. 2). As a negative control, prey MalE-PsbQ was loaded in a control column prepared with the soluble protein fraction of *Escherichia coli* harbouring the empty expression vector. This column did not retain MalE-PsbQ.

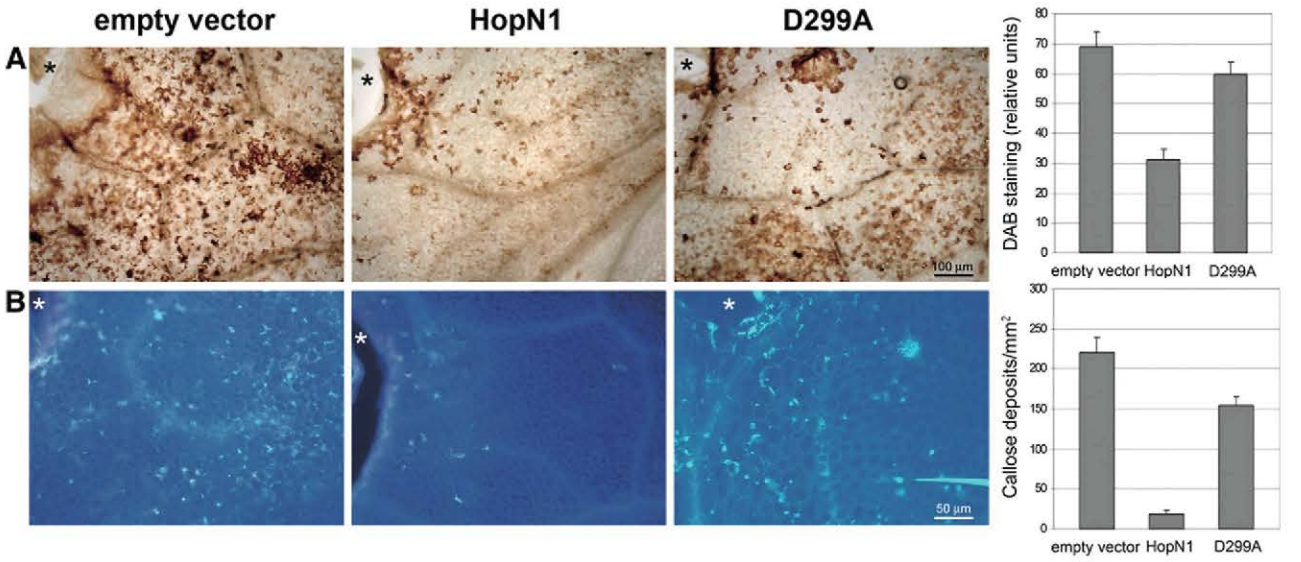

Fig. 1. DAB staining and callose deposition in *Arabidopsis* leaves. *Arabidopsis* plants were challenged with Pf55(pLN18) harbouring the pCPP5040 empty vector, or the vector expressing HopN1 protein or the catalytic mutant $HopN1_{D299A}$.
A. DAB signal was quantified 4 h after infection (see Table S1) and represented in a histogram.
B. Callose deposition was detected by aniline blue staining and quantified (see Table S1) 12 h after infection (Wound, asterisk).

Previously, Dowen and coworkers (2009) observed a punctuate staining of HopN1 in the plasma membrane of Chinese cabbage epidermal cells as well as in tobacco epidermal cells through transient expression using particle bombardment. To further explore HopN1 localization, we transiently transformed onion (*Allium cepa*) epidermal cells by particle co-bombardment using HopN1–GFP fusions and a subcellular marker for plastids fused to RFP. Figure S3 shows the colocalization of HopN1 with the marker for plastids, which strongly supports the chloroplast location of HopN1 in green tissues. To determine if the HopN1 subcellular location in green tissues was compatible with this suggested target, we transiently transformed *Nicotiana benthamiana* leaves by agroinfiltration of a HopN1–GFP fusion. Figure 3A shows that HopN1 localized to chloroplasts in intact tissues, and Fig. 3B shows the localization in isolated chloroplast. To verify the precise localization in thylakoid samples we carried out subcellular fractionation of *N. benthamiana* leaves previously infiltrated with Pf55(pLN18) expressing HopN1. The presence of HopN1, detected by immunoblot analysis, in the thylakoid fraction of plants infected with Pf55(pLN18) expressing HopN1 demonstrates its physical colocalization with PsbQ in this cellular compartment. Bacterial contamination of plant chloroplast preparations was discarded by using an antibody against the *P. fluorescens* OprL protein (Hancock *et al.*, 1990). OprL (Pal) is a highly conserved and abundant structural membrane protein in Gram-negative bacteria (i.e. its number has been calculated to be ≈30 000–40 000 copies/cell in *E. coli*) (Cascales *et al.*, 2002). No OprL protein was detected in

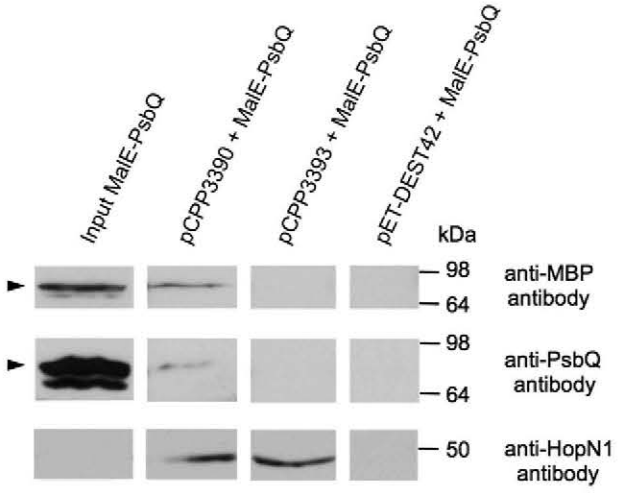

Fig. 2. *In vitro* pull-down assay with purified MalE-PsbQ and HopN1-His_6 tagged proteins. Immunoblot analyses of the eluted fractions from different columns loaded with the MalE-PsbQ purified protein are shown. The Ni-NTA agarose columns contained soluble bacterial protein extracts from *E. coli* BL21(DE3) expressing the wild-type HopN1-His_6 tagged protein (pCPP3390), the HopN1-D299A-His_6 (pCPP3393), or harbouring the empty expression vector (pET-DEST42). The membranes were hybridized with anti-MBP antibody (upper panel), anti-PsbQ antibody (middle panel) or anti-HopN1 antibody (lower panel). Samples of purified MalE-PsbQ were also included in the gels as a positive control. The presence of a lower band in the input samples is probably due to the presence of minor amounts of MalE after the cleavage of its signal peptide. The presence of a differential band (see arrowhead) when probed with the anti-MBP antibody or the anti-PsbQ antibody, which specifically co-eluted with the HopN1-His_6 tagged wild-type protein, demonstrates the physical interaction between PsbQ and HopN1.

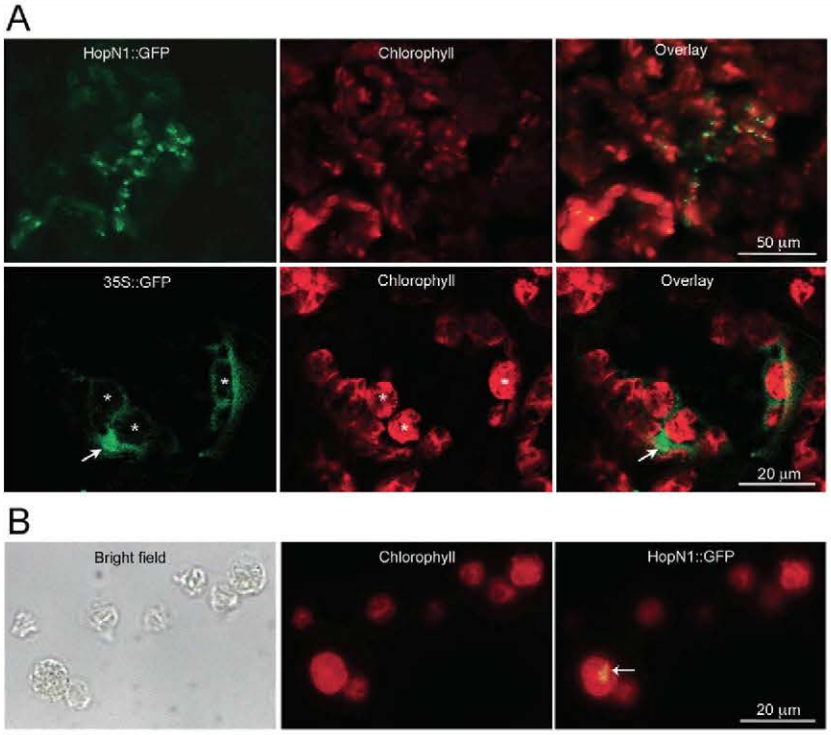

Fig. 3. Subcellular localization of HopN1::GFP in *N. benthamiana* leaves.
A. Transient expression in *N. benthamiana* leaves was achieved by agroinfiltration using plasmids harbouring the constructs HopN1::GFP and 35S::GFP. Projections of stacks of optical sections were collected on a confocal microscope under excitation with the laser lines of 488 nm (GFP) and 633 nm (chlorophyll). HopN1::GFP is observed as a diffuse signal and some brighter foci inside the chloroplasts, which exhibit natural red autofluorescence. The labelling pattern is strikingly different from the intense signal of 35S::GFP, which homogeneously covers wide cytoplasmic areas (arrow) and excludes the chloroplasts (asterisks).
B. Chloroplasts were purified from *N. benthamiana* leaves 48 h after agroinfiltration of *A. tumefaciens* harbouring the HopN1::GFP construct. Observation of the subcellular fractions in a light microscope under bright field revealed the purity of the preparation, which lacked contamination with other organelles. The chloroplasts were also identified by the red autofluorescence of the chlorophyll using the following filters set: BP 546, FT 580, LP 590. The rightmost image shows the presence of HopN1::GFP fluorescence in one chloroplast (arrow) when the preparation was excited with blue light. The filter combination available (450–490, FT 510, LP 520) also permits the simultaneous collection of chlorophyll red autofluorescence. This picture is representative of 15 similar observations from two independent agroinfiltration experiments.

these preparations, confirming that HopN1 presence was not due to bacterial contamination (Fig. 4).We carried out several attempts to show the proteolytic activity *in vitro* using the purified recombinant proteins but with no success, probably due to the difficulty in mimicking *in vitro* the native physiological conditions of the activity. However, we were able to observe the *in vitro* proteolysis using *N. benthamiana* thylakoids samples and partially purified HopN1 protein (Fig 5).

HopN1 interferes with PSII activity

To analyse the effect of HopN1 on the function of PSII we performed ferricyanide Hill reaction analysis. These assays enable quantification of non-cyclic photoelectron transport, and consequently O_2 production, by measuring ferricyanide photoreduction. We challenged tomato plants with Pf55(pLN18) expressing HopN1, and after 3 h we performed this analysis in chloroplast preparations of the challenged tomato leaves. Although there was a high variability in these experiments, in all cases we detected reduction in the activity of PSII in the chloroplast samples of plants expressing HopN1 (Fig. 6 and Table S2). These results suggest that the proteolysis of PsbQ by HopN1 diminishes the photolysis of water and therefore also both oxygen production and electron transport.

Silencing NtPsbQ *expression or deploying HopN1 reduces bacterium-induced ROS generation and plant cell death, but HopN1 does not contribute to bacterial growth* in planta

To further test the role of PsbQ in plant responses to bacteria, *NtPsbQ*-silenced tobacco plants were challenged with Pf55(pLN18) harbouring HopN1 or an empty expression vector (Fig. 7 and Table S3). Silencing *NtPsbQ* led to a significant decrease in ROS production following inoculation with the empty vector control. HopN1

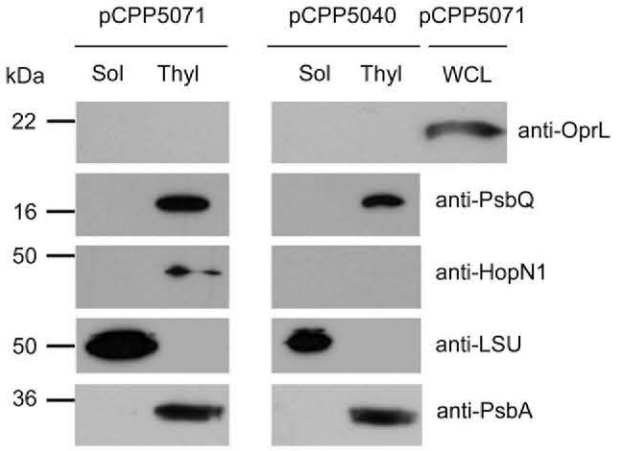

Fig. 4. Subcellular localization of HopN1 in *N. benthamiana* thylakoids after infection with *P. fluorescens* 55(pLN18) expressing HopN1. *N. benthamiana* plants were challenged with 100 µl of a suspension of 1×10^8 cfu ml^{-1} of Pf55(pLN18) expressing the HopN1 protein (pCPP5071) or harbouring the empty vector (pCPP5040). Sixteen hours after inoculation, leaf tissues were collected, homogenized and used for chloroplast isolation and further thylakoid purification. Thylakoid fractions (Thyl, 20 µg of total protein/lane) and soluble protein fraction (Sol, 5 µg of total protein/lane) were run on 17.5% SDS-PAGE gels and analysed by immunoblotting using polyclonal antibodies raised against PsbQ, HopN1, RbcL (large subunit of Rubisco, LSU) or the PsbA protein. The last two antibodies were used as a control for the purity of the different cellular fractions. As an additional control, the above samples were also analysed by immunoblotting with a monoclonal antibody directed against the OprL (Pal) protein of *P. fluorescens* [WCL, whole-cell lysate of Pf55(pLN18) harbouring pCPP5071].

suppressed ROS production in the challenged WT tobacco plants, but caused no further reduction in ROS in *NtPsbQ*-silenced plants.

We reported earlier that HopN1 suppresses PCD associated with the non-host HR elicited by *PsPto* in tobacco

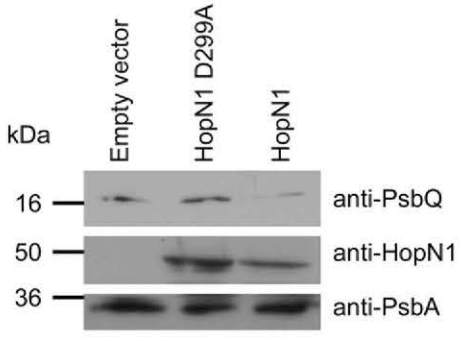

Fig. 5. *In vitro* proteolysis of PsbQ by HopN1. Thylakoid samples from *N. benthamiana* plants containing PsbQ were incubated in the presence of soluble cell lysates of *E. coli* BL21 (DE3) carrying the pET-DEST42 plasmid (empty vector) or expressing wild-type HopN1 protein (pCPP3390) or its non-catalytic HopN1D299A mutant version (pCPP3393). Samples were analysed by immunoblotting using anti-PsbQ and anti-HopN1 antibodies. The immunoblot with the antibody directed against PsbA (thylakoid marker) was used to check for equal loading of the thylakoid protein samples.

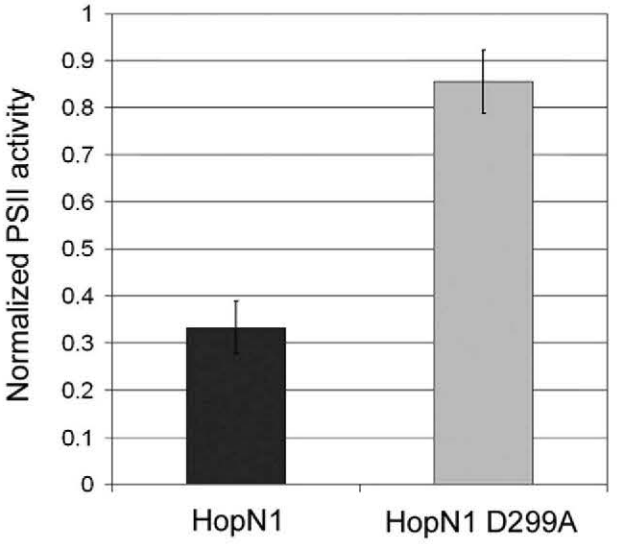

Fig. 6. PSII activity in isolated tomato chloroplasts. O_2 production in tomato chloroplast samples was estimated by quantification of ferricyanide photoreduction. Tomato leaves were inoculated with Pf55(pLN18) harbouring the empty vector or expressing the HopN1 protein or the mutant derivative. Values are the mean and standard error of three experiments and are expressed as PSII relative activity, where the PSII activity (µmol O_2 mg^{-1} chlorophyll·h) was normalized to that recorded in the samples from plants inoculated with Pf55(pLN18) harbouring the empty vector. Raw data are shown in Table S2.

plants (López-Solanilla *et al.*, 2004). To determine if this phenomenon is related to the targeting of PsbQ, we inoculated tobacco leaves (WT and *NtPsbQ*-silenced) with *PsPto* (WT and *hopN1* mutant strains). As expected, we could detect a threshold level of inoculum (3×10^6 cfu ml^{-1}) where the *hopN1* mutant strain produced a larger necrosis than the WT strain. However, we also found that the HR and associated electrolyte leakage from inoculated leaf tissue were reduced in the *NtPsbQ*-silenced plants, independently of the inoculated bacterial strain, as indicated by the need to increase the inocula by one order of magnitude (to 1.3×10^7 cfu ml^{-1}) to elicit the HR (Fig. 7C). In tobacco, the DC3000 *hopN1* mutant produced a stronger HR than the wild-type strain. Thus, both silencing of *NtPsbQ* and catalytic inactivation of *hopN1* indicate that PsbQ quantitatively contributes to the ROS elicited by Pf55(pLN18) and the PCD elicited by *PsPto.* We previously observed that the inactivation of *hopN1* in *PsPto* DC3000 caused a reduction in symptom development without affecting growth in tomato (López-Solanilla *et al.*, 2004). However, it is possible that a potential contribution of HopN1 to bacterial growth *in planta* might be masked by functional redundancy with linked effector genes in the *PsPto* conserved effector locus (CEL). Therefore, we used DC3000 mutant CUCPB5501 (Kvitko *et al.*, 2009), which has a deletion affecting *hopQ1-1* and the CEL-linked effector genes, *avrE*, *hopM1*, *hopAA1-1*

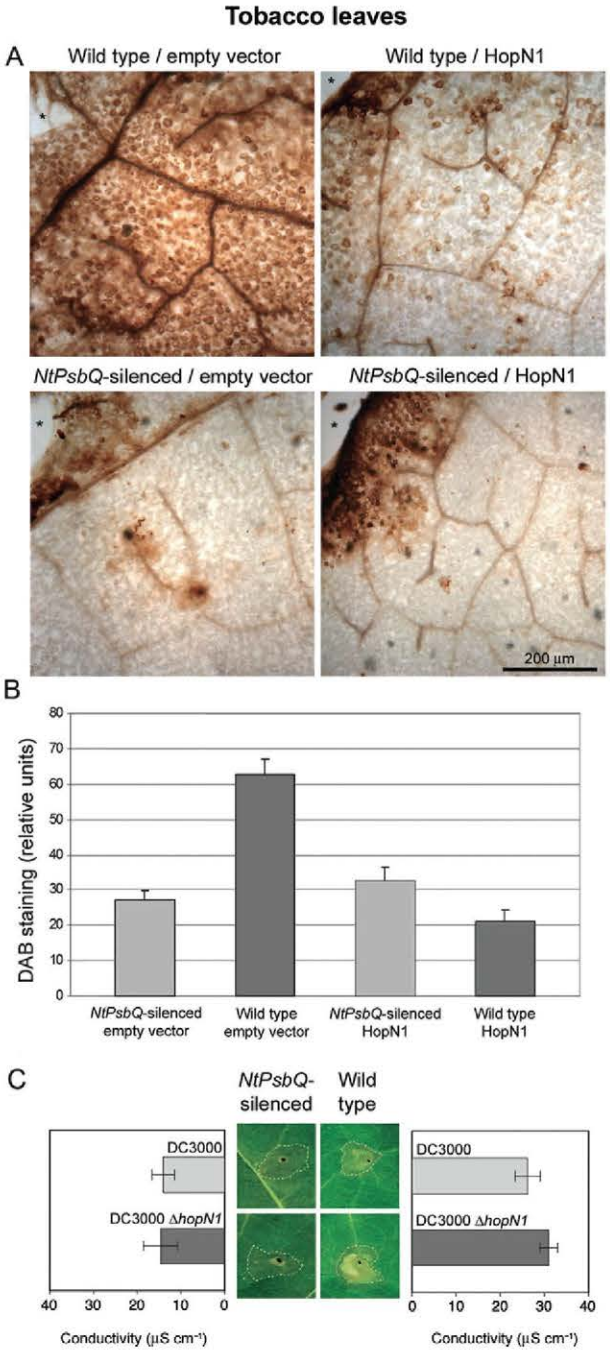

Fig. 7. ROS production and HR elicitation in *NtPsbQ*-silenced plants.
A. WT and *NtPsbQ*-silenced tobacco plants were challenged with 100 µl of a suspension of 1×10^8 cfu ml^{-1} of Pf55(pLN18) expressing the HopN1 protein or harbouring the empty vector. ROS production was detected 4 h after infection by DAB staining (Wounds, asterisks).
B. Histogram representing the quantification of DAB signal from the specimens shown in panel (A). Raw data can be found in Table S3.
C. HR elicitation. DC3000 and the DC3000 *hopN1* mutant were infiltrated into tobacco leaves with a dilution series of inoculum (from 1×10^6 to 2×10^8 cfu ml^{-1}). Twenty-four hours later, leaves inoculated at the threshold level of inoculum for HR elicitation (3×10^6 cfu ml^{-1} for WT plants and 1.3×10^7 cfu ml^{-1} for *NtPsbQ*-silenced plants) were photographed. Then, equal amounts of the infiltrated areas were excised and vacuum infiltrated in 10 ml of H_2O, shaken for 1 h at room temperature. Electrolyte leakage was measured by recording conductivity of the sample solutions after removing the leaf discs. Values given represent the mean and standard error from three leaves obtained from different plants. The means of wild-type plants challenged with DC3000 or with the *hopN1* mutant were different from the means of *NtPsbQ* plants challenged with the same strains according to the one-way ANOVA ($\alpha = 0.05$) Fisher LSD method with the following *P*-values (WT plants-DC3000 vs *NtPsbQ* plants-DC3000 $P = 0.019$, WT plants-DC3000 vs *NtPsbQ* plants-*hopN1* $P = 0.024$, WT plants-*hopN1* vs *NtPsbQ* plants-DC3000 $P = 0.003$, WT plants-*hopN1* vs *NtPsbQ* plants-*hopN1* $P = 0.004$).

and *hopN1*. HopQ1-1 functions as an avirulence determinant in *N. benthamiana* (Wei *et al.*, 2007), and a desirable characteristic of *hopQ1-1* mutants is that they can successfully infect *N. benthamiana*, which is a model plant that is particularly useful for detecting slight differences in bacterial growth and symptom production (Cunnac *et al.*, 2011). We then restored HopN1 production to this mutant using a cloned *hopN1* gene expressed from a *hrp* promoter, and tested CUCPB5501 derivatives carrying *hopN1* or an empty vector for growth and symptom production in *N. benthamiana*. The production of HopN1 reduced necrotic lesion formation by CUCPB5501 but did not stimulate bacterial growth *in planta* (Fig. 8). To further reduce the potential for effector redundancy, we examined the effect of HopN1 on growth and chlorotic symptom formation in *N. benthamiana* by CUCPB6031. This strain is a derivative of DC3000 in which all 28 of the well-expressed effector genes have been deleted and a minimal set of five effectors (AvrPtoB, HopM1, HopE1, HopG1 and HopAM1) capable of promoting modest growth and chlorotic symptoms at 10^5 cfu ml^{-1} was restored. The addition of HopN1 altered neither growth nor symptom production by CUCPB6031 (Fig. 8).

Discussion

Reactive oxygen species production takes place during the activation of both PTI and ETI (Doke and Ohashi, 1988; Piedras *et al.*, 1998; Felix *et al.*, 1999; Torres *et al.*, 2002; Krause and Durner, 2004; Kaku *et al.*, 2006), and this is proposed to be one of the overlapping aspects of both responses (Oh *et al.*, 2010; Tsuda and Katagiri, 2010). The results obtained in this work show how the effector protein HopN1 blocks ROS production, an activity that likely explains the previously observed HopN1-mediated inhibition of cell death associated with the HR (López-Solanilla *et al.*, 2004). Our results also indicate that the mechanism underlying this inhibition is HopN1-dependent disruption of ROS production in the chloro-

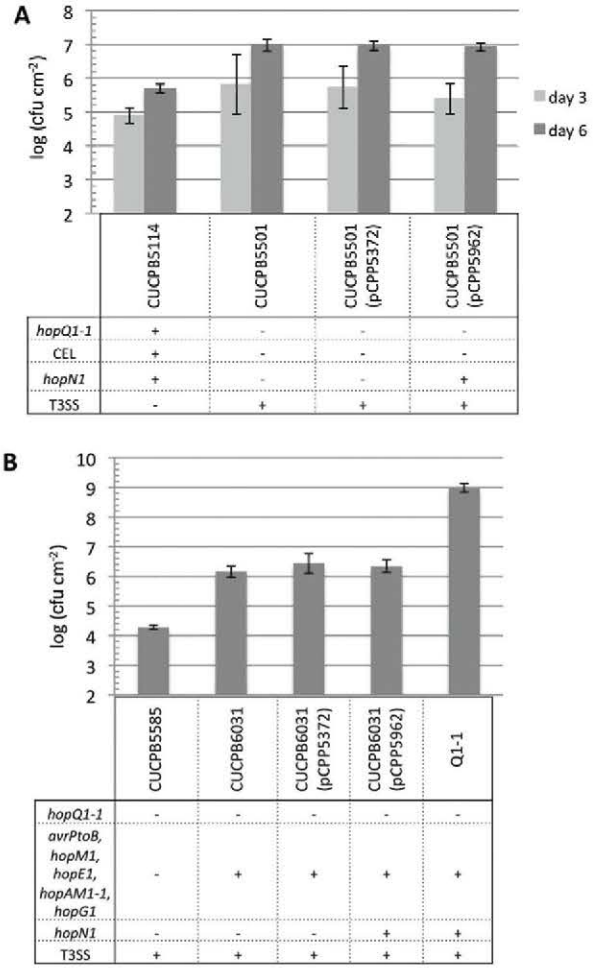

Fig. 8. Effect of HopN1 on the ability of *P. syringae* pv. *tomato* DC3000 derivatives lacking multiple type III effector genes to grow and produce symptoms in *N. benthamiana*. CUCPB5501 and CUCPB6031 were complemented with HopN1 using the plasmid pCPP5962 (P_{avrPto}-*shcN-hopN1*-HA), and pCPP5372 was used as an empty vector control. Growth and symptom development were assessed in *N. benthamiana* leaves.

A. CUCPB5501 does not show any increase in growth when complemented with HopN1 at two time points following inoculation at 3×10^4 cfu ml^{-1}.

B. CUCPB6031, which contains the five effectors indicated in the grid below the graph, does not show any increase in growth in the presence of HopN1 6 days after inoculation at 3×10^4 cfu ml^{-1}. The effectorless mutant CUCPB5585 and DC3000Δ*hopQ1-1* were used as controls. The average log (cfu cm^{-2}) along with standard deviation from 3–6 plants per strain is shown. The experiments were repeated at least twice with similar results.

C. Symptom production was evaluated in leaves inoculated with the indicated strains, and representative photographs from one experiment are shown. CUCPB5501 (left-hand side panel) shows reduced lesion formation in the presence of HopN1 when inoculated at 3×10^5 cfu ml^{-1} in 7 out of 12 spots. This was determined to be significant using Fisher's exact test ($\alpha = 0.05$). The photographs were taken 5 days after inoculation. CUCPB6031 (right-hand side panel), which normally causes mild chlorosis when inoculated at 1×10^5 cfu ml^{-1}, does not show altered symptoms in the presence of HopN1 in any of the spots tested. The photographs were taken 6 days after inoculation. The number of spots showing the symptoms depicted in the photographs, out of the total number of spots inoculated, is given. The experiments were repeated three times with similar results.

plast. The inhibition of ROS production is clearly dependent on a catalytically active HopN1 protein, although this activity might not be completely abolished in the non-catalytic mutant protein assayed here ($HopN1_{D299A}$), which appears to still retain residual proteolytic activity (López-Solanilla *et al.*, 2004).

In this work we have shown that HopN1 colocalizes and interacts with PsbQ, a protein of the OEC of PSII. These results together with the observed HopN1-dependent PsbQ decrease strongly indicate that this protein is a natural target for this *PsPto* effector protein.

The identification of the plant target of HopN1, PsbQ, reveals that this protein is required for full deployment of ROS and ROS-associated defences, such as PCD (HR) and callose deposition. PsbQ is an extrinsic protein of the OEC of PSII, which has been previously associated with stress conditions in higher plants (Coker *et al.*, 2005; Ifuku *et al.*, 2005; Yi *et al.*, 2006). *NtPsbQ*-silenced plants show normal photosynthetic activity under normal light conditions but the efficiency is altered under low light conditions (Ifuku *et al.*, 2005; Yi *et al.*, 2006).

We have observed an alteration of the photoelectron transport in preparations from HopN1-expressing leaves. The observed suppression of ROS production by HopN1 could be due directly or indirectly to the effect on the OEC. Consequently, our results point to a general role of PsbQ in maintaining photosynthetic activity during stressful conditions, including infection by a plant pathogen. We also showed that the integrity of PsbQ is needed to fully trigger plant immune responses against *PsPto*, highlighting the contribution of the photosynthetic pathway to plant defence responses. A few studies have shown protein variation in the OEC associated with viral infections, as it occurs in peanut plants infected with peanut green mosaic virus (Naidu *et al.*, 1986), tobacco plants infected with cucumber mosaic virus strain Y (CMV-Y) (Takahashi *et al.*, 1991; Takahashi and Ehara, 1992), and *Nicotiana* plants infected by Tobamoviruses (Pérez-Bueno *et al.*, 2004). Additionally, Abbink *et al.* (2002) showed that silencing of PsbO (33 kDa OEC protein) enhanced virus replication in *Nicotiana* plants. Moreover, Jones *et al.* (2006) identified modifications in the abundance of OEC

proteins during R-gene-mediated HR in *Arabidopsis* plants infected with *PsPto*, suggesting that resistance mechanisms utilize or modify PSII. Although the specific mechanisms underlying these phenomena have been elusive, our results offer an explanation, suggesting that the photosynthesis apparatus is participating in a general defence response against different types of invading pathogens, and that these are able to manipulate this response to their advantage by shutting down the generation of harmful ROS. In this line, it has been previously described that coronatine (COR) targets photosynthetic machinery to modulate chloroplast ROS homeostasis in promoting disease-associated cell death during bacterial speck disease of tomato (Ishiga *et al.*, 2009a,b). In addition, recent results from Ishiga *et al.* (2011) indicate that NTRC (NADH dependent thioredoxin reductase C) and Prx (2-Cys peroxiredoxin C), the central players of chloroplast redox detoxification system, function as negative regulators of pathogen-induced cell death in plant healthy tissues that surround the lesions. In this work it is also shown that induced chloroplasts-localized ROS play a role in enhancing the disease-associated cell death. Loss-of-function analysis of Prx and NTRC resulted in spreading accelerated *PsPto* disease-associated cell death with enhanced ROS accumulation in a COR-dependent manner in tomato and *Arabidopsis*. Interestingly authentic COR suppressed the expression of Prx and NTRC in tomato but not in *Arabidopsis*, suggesting that COR in conjunction with other effectors may modulate ROS and cell death in different host species.

The cellular origins of ROS are still a subject of controversy. Plasma membrane NADPH oxidase has been proposed as the main source for the apoplastic oxidative burst in most plant–pathogen interactions (Torres and Dangl, 2005). However, high levels of ROS can be produced by different enzymatic activities in other compartments of the cell, and light conditions were also shown to influence specific defence responses (Zeier *et al.*, 2004; Padmanabhan and Dinesh-Kumar, 2010). Additionally, it has been recently reported that chloroplast-generated ROS play a major role in localized cell death during the interaction of tobacco plants with pathogens such as TMV (Liu *et al.*, 2007) and *Xanthomonas campestris* pv *vesicatoria* (Zurbriggen *et al.*, 2009). Our findings using *NtPsbQ*-silenced plants, where the non-host HR elicited by *PsPto* was drastically reduced, are in line with the above-mentioned reports. More interestingly, *PsPto* has evolved a mechanism for the specific manipulation of the production of chloroplast ROS, which highlights the relevance of the photosynthesis-derived oxidative stress in plant defence against bacterial pathogens.

The photosynthetic machinery within the chloroplast has been reported to be a source of ROS, and this activity was associated with the plant response to stress (Piñas-Fernández and Strand, 2008; Padmanabhan and Dinesh-Kumar, 2010). In fact, plant defence against pathogen infection has been shown to be linked to the light-sensing network and to the oxygen-evolving complex in PSII (Abbink *et al.*, 2002; Genoud *et al.*, 2002). From our data, we cannot establish how PsbQ proteolysis affects the whole photosynthetic machinery, but it is known that PsbQ is essential to maintain and improve the function of the PSII under stress conditions (Coker *et al.*, 2005; Ifuku *et al.*, 2005; Yi *et al.*, 2006). Our hypothesis correlates with that raised by Liu *et al.* (2007): upon pathogen/PAMPs recognition the plant cell initiates a cascade of signals involving MAPKK and this cascade inhibits carbon fixation in the chloroplast, which creates a situation of excess excitation energy in plants under illumination, resulting in the generation of ROS in the chloroplast. The excess of excitation energy could be recognized as a stress condition that destabilizes the PSII. Under these conditions, PsbQ could be involved in the stabilization of the PSII (as has been described under other types of stress), thus becoming a key element in maintaining or even enhancing the production of ROS in this situation. HopN1 activity would interfere with the enhancement/stabilization of this machinery, making the pathway less effective, which would lead to a decrease in ROS production from the chloroplast.

PsPto HopN1 appears unique among the effectors of plant–pathogenic bacteria in targeting PSII. However, the J-domain protein HopI1 of *P. syringae* pv *maculicola*, causing remodelling of thylakoids and the suppression of SA accumulation, may have a similar effect (Jelenska *et al.*, 2007).

An intriguing aspect of our findings is that HopN1-mediated degradation of PsbQ reduces early immunity responses, such as ROS generation and callose formation, and late responses, such as cell death and electrolyte leakage, without any apparent effect on bacterial growth. How effectors in a repertoire work together or redundantly to promote growth and symptom production is poorly understood, but the recent development of *P. syringae* pv. *tomato* DC3000 derivatives with variously disassembled or reassembled effector repertoires is providing new tools to address this issue (Cunnac *et al.*, 2011). By using such DC3000 derivatives we learned that HopN1 makes no contribution to bacterial growth in *N. benthamiana* even when expressed in a partially disassembled DC3000 derivative lacking the CEL effectors or when expressed in a DC3000 derivative with a partially reassembled repertoire of five effectors that restores modest growth in *N. benthamiana*.

However, HopN1 does have a significant role in regulating the production of necrotic disease symptoms. HopN1 expressed in bacteria or transgenically *in planta* can diminish the cell death elicited by DC3000 in tomato

(López-Solanilla *et al.*, 2004), by *P. syringae* pv. *tabaci* in tobacco (López-Solanilla *et al.*, 2004), by Pf55(pHIR11) expressing HopA1, an ETI-elicitor, in tobacco (Guo *et al.*, 2009), and by a DC3000 Δ*hopQ1-1*ΔCEL derivative in *N. benthamiana* (this work). These observations suggest that HopN1 can suppress the cell death elicited by many *P. syringae* effectors and more generally that HopN1-dependent destruction of PsbQ has a broad ability to reduce pathogen-induced cell death. In summary, our findings highlight the importance of light and multiple sources of ROS in bacterium–plant interactions, particularly in disease-associated cell death, and they suggest that components of the photosynthetic apparatus could constitute novel targets to improve the ability of plants to tolerate bacterial infections with reduced symptoms.

Experimental procedures

Bacterial strains, plasmids, culture media and growth conditions

Bacterial strains and plasmids used in this study are listed in Table S4. *E. coli* was grown in Luria–Bertani broth at 37°C. *Pseudomonas* sp. strains were routinely grown in King's B (KB) medium (King *et al.*, 1954) at 30°C. When required, antibiotics were used at the following final concentrations (in μg ml^{-1}): ampicillin, 100; chloramphenicol, 30; gentamicin, 25; hygromycin, 50; kanamycin, 50; rifampicin, 50; spectinomycin, 25; and tetracycline, 20.

Plant materials

Tomato plants (*Solanum lycopersicum* cv. Moneymaker) were between 3 and 4 weeks old, *Nicotiana tabacum* cv. Xanthi plants were between 4 and 6 weeks old, and *Arabidopsis* Col-0 plants were 4 weeks old. *NtPsbQ*-silenced tobacco plants were selected with kanamycin as previously described and their phenotype confirmed by immunoblotting (Fig. S4) (Ifuku *et al.*, 2005). All plants were grown in greenhouse conditions at 24/22°C (day/night) with 10 h light (110 μmol m^{-2} s^{-1}) and relative humidity of 65%.

Plant bioassays

Plant materials and culture conditions are described in *Supporting information Experimental procedures*. For HR assays, tobacco leaves were inoculated by infiltrating serial dilutions of bacterial suspensions, and infiltrated areas were excised from the leaves. Electrolyte leakage was determined as described (López-Solanilla *et al.*, 2004). Assays with Pf55(pLN18) derivatives were performed by infiltrating a bacterial suspension (1×10^8 cfu ml^{-1}) into plant leaves using a blunt syringe.

Detection of ROS production and callose deposition

DAB staining was performed according to Thordal-Christensen *et al.* (1997). Callose deposition was stained as described in Guo *et al.* (2009). Four hours after bacterial inoculation, either entire *Arabidopsis* leaves or small pieces of tomato and tobacco leaves, cut around the injection area, were stained by pressure infiltration in a freshly prepared 1 mg ml^{-1} solution of 3,3′-diaminobenzidine (DAB, Sigma-Aldrich D-8001) in 8 mM HCl, pH 3.8. Chlorophyll was removed by submerging the leaves into a solution of ethanol/lactic acid/glycerol [3:1:1 (vol/vol/vol)] at 60°C, then kept overnight at room temperature on water-soaked filter paper. At least six biological replicas from each specimen were mounted on slides in a solution of 40% (vol/vol) glycerol and observed with a Zeiss Axiophot microscope under bright field. DAB staining produces a precipitate of an intense brown colour in those areas where ROS was generated, next to the infection zone. Callose deposition was developed 12 h after inoculation. Chlorophyll was removed in 95% (vol/vol) ethanol and staining was performed in a 0.02% (wt/vol) solution of aniline blue (Sigma-Aldrich #415049) in 150 mM potassium phosphate, pH 9 for 1 h in darkness. At least six biological replicas from each specimen were mounted in 40% (vol/vol) glycerol on glass-slides. Observations were carried out under UV light excitation using the filter cube (BP365, FT 395, LP 397) on a Zeiss Axiophot fluorescence microscope. For quantification of ROS production and callose deposition, up to four snapshots of each specimen from equivalent areas surrounding the wound (inoculation zone) were captured with a Leica DFC 300FX CCD colour camera using the Leica Application Suite 2.8.1 build 1554 acquisition software. The same settings (exposition time, colour saturation and gamma) were applied to all samples.

Quantification of DAB staining and aniline blue fluorescence

To analyse the intensity of DAB staining, the images were taken at a final magnification of 50×. Quantification was performed with the aid of the program Image J (http://rsb.info.nih.gov/nih-image/). The brown colour of the precipitate was separated by colour deconvolution with the methyl green DAB vector to discard the background. Then, the corresponding channel was used to measure the intensity of the signal. The average values and standard deviations for each specimen were calculated on MS Excel from the quantified snapshots. Because in 8 bit images (256 grey levels) the intensity value 0 corresponds to the black colour and 255 to white, the lower the average values the darker the staining. Thus, to represent the relative intensity of DAB staining referred to the control (specimens treated with $MgCl_2$) in a histogram and facilitate comparisons, a positive correction was applied by subtracting 255 to the average values. Then, the higher the relative value in the histogram the higher the intensity of DAB staining and, therefore, ROS production. Standard error was calculated according to the formula $SE = SD/\sqrt{n}$ (n = number of samples). To analyse aniline blue fluorescence the images were taken at a final magnification of 100× for a better identification of the labelling. To quantify callose staining the images were divided in squares of 838 μm^2 by overlapping a grid onto the pictures using the program ImageJ. The number of squares containing specific fluorescence (either foci or continuing lines extending for some μm along the cell walls) was counted and the results were referred to the total area expressed as mm^2, according to the standard nomenclature found in the literature. The original data were corrected by subtracting the number of fluorescent squares in leaves treated only with $MgCl_2$, as a measure of background. SE was calculated as described above.

Pull-down assays using plant extracts and liquid chromatography analysis

Escherichia coli BL21 (DE3) (pCPP3390) expressing HopN1-His_6 was grown at 25°C to an OD_{600} of 0.6 and then induced with 0.5 mM isopropyl β-D-thiogalactoside (IPTG) for 3 h. Cells were harvested by centrifugation (4000 *g*, 20 min). The protocol recommended for native protein purification in the QIAExpressionist Handbook was followed, introducing an additional incubation step with a tomato leaf extract for 1 h at 4°C before the elution step. The tomato leaf extract was obtained by grinding 5.17 g of tissue in 75 ml of lysis buffer (50 mM NaH_2PO_4, 300 mM NaCl, 10 mM imidazole, pH 8.0). As a control the same protocol was carried out starting with a culture of *E. coli* BL21 (DE3) harbouring the empty vector. Lyophilized eluted samples were dissolved in denaturing buffer [6 M urea, 10% (vol/vol) glycerol, 25 mM Bis-Tris, 0.2% (wt/vol) n-octylglucoside]. The solution was vortexed and centrifuged (16 500 *g* at 4°C, 15 min). The supernatant was filtered through a 0.2 μm sterile filter. Protein quantification was performed by using the microBCA protein assay reagent kit (Pierce #23227). The samples were further resolved by liquid chromatography analysis and the differential peaks obtained were subjected to MS (see *Supporting information*). This experiment was done three times and similar results were obtained regarding the differential peaks in the chromatograms.

In vitro *pull-down assays*

Escherichia coli BL21 (DE3) cells containing the appropriate vectors were grown at 37°C, 200 r.p.m. in 400 ml of 2xYT medium until an OD_{600} of 0.5. Cell cultures carrying the control vector or expressing the MalE-PsbQ fusion or the HopN1-His_6 derivatives were induced with 1 mM IPTG and further incubated for 4 h. Cells expressing the His-tagged proteins were then collected and disrupted by sonication at 4°C, and the cell extracts were adsorbed to Ni-NTA agarose beads as recommended by the manufacturer (QIAGEN, Cat. No. 31314). Cells expressing the MalE-PsbQ fusion were disrupted using the B-PER bacterial protein extraction reagent (Pierce Cat. No. 78243), and the soluble fraction was purified using amylose resin following manufacturer's recommendations. The eluted MalE-PsbQ fusion protein was loaded onto the Ni-NTA agarose columns previously loaded with the HopN1-His_6 extracts, and incubated for 1 h at 4°C. After washing the columns with buffer (50 mM NaH_2PO_4, 300 mM NaCl, pH 8.0) containing increasing amounts of imidazole (10 and 20 mM), the HopN1-His_6 tagged recombinant proteins were finally eluted with 1 ml 250 mM imidazole. The resulting fractions were dialysed against deionized water o/n at 4°C using a Spectra/Por membrane (MWCO: 6–8000, Spectrum Laboratories) and concentrated by lyophilization. Samples were run on SDS-PAGE and immunoblotted with anti-HopN1, monoclonal anti-MBP (Sigma, SAB4200082) or polyclonal anti-PsbQ (Abcam, ab65568) antibodies. HopN1 rabbit polyclonal antibody was generated against the complete His_6 recombinant protein using standard methods (Pocono Rabbit Farm, Canadensis, PA). Blots were incubated with a 1:40 000 (anti-HopN1), 1:20 000 (anti-MBP) or 1:1000 (anti-PsbQ) dilutions of the antibodies. Goat anti-rabbit IgG conjugated to HRPO was used (1:20 000) as secondary antibody against anti-HopN1 and anti-PsbQ antibodies. Anti mouse IgG1 (SantaCruz) (1:20 000) was used as secondary antibody against anti-MBP. The Immobilon Western Chemiluminiscent HRP substrate (Millipore) was used for detection following manufacturer's directions.

Thylakoid isolation, chlorophyll determination and photochemical activities

Tomato leaves samples (1.5–3 g fresh weight) from plants challenged with the Pf55 strains harbouring the desired construction were collected 2 h after infection. The tissue samples were ground in a mortar, chilled with liquid nitrogen, with 20 ml of 2% (wt/vol) NaCl. The homogenate was filtered through two layers of gauze and centrifuged at 100 *g* for 2 min. The supernatant was centrifuged again at 1000 *g* for 10 min. The chloroplast preparations obtained were resuspended in 10 ml of 0.2% (wt/vol) NaCl using a cotton stick. This thylakoid suspension was kept at 4°C in darkness. Total chlorophyll was determined as described (Arnon, 1949). The Hill reaction using ferricyanide as an electron acceptor was performed by following the reduction as the decrease in absorbance at 420 nm using 100 W incandescent light with an intensity of 560 μmol m^{-2} s^{-1} as light source.

Intact chloroplasts of *N. benthamiana* leaves were obtained as previously described by Aronsson and Jarvis (2002), using a Percoll linear gradient. Organelle purity was monitored via bright field and fluorescence microscopy. Thylakoid and stroma fractions were obtained as follows: a sample of intact chloroplasts was centrifuged at 12 000 *g* for 5 min at 4°C and the pellet was resuspended in lysis buffer (62.5 mM TrisCl pH 7.5, 2 mM $MgCl_2$) and incubated on ice for 15 min. After that, the sample was centrifuged at 12 000 *g* for 5 min at 4°C. The supernant containing the soluble fraction was collected and the pellet containing the thylakoid fraction was resuspended in lysis buffer. Protein concentration of each sample was determined by BCA assay.

Subcellular localization of HopN1

Agrobacterium construct (pGWB5-GFP-HopN1) was made by Gateway technology. The constructs used in the present study were introduced into *Agrobacterium tumefaciens* strain GV3101 by electroporation (Weigel and Glazebrook, 2002). Overnight cultures of recombinant *A. tumefaciens* were used to inoculate 100 ml of YEB medium supplemented with 50 μg kanamycin, 50 μg rifampicin and 20 μg gentamicin per millilitre and 0.2 mM of acetosyringone. Cells were grown until exponential phase (OD_{600} = 0.6–0.8), harvested by centrifugation and resuspended in MMA buffer supplemented with acetosyringone to reach an optical density of 2.1–3. Cultures were incubated at room temperature for 1 h before infiltration. Four leaves of *N. benthamiana* plants were infiltrated with the *A. tumefaciens* cultures using a 1 ml syringe. Fluorescence images were acquired using a confocal microscope (LEICA-Sp5).

The same plants were subjected to the chloroplast isolation procedure described above. Intact chloroplasts from *N. benthamiana* leaves infected with *A. tumefaciens* pGWB5-GFP-HopN1 were monitored via fluorescence microscopy to verify the presence of HopN1–GFP in the chloroplast. To confirm the subcellular localization of HopN1, *N. benthamiana* leaves infected with Pf55(pLN18) expressing HopN1 as described above, were also subjected to chloroplast isolation. Thylakoid, and soluble fractions corresponding to stroma and cytoplasm were obtained and analysed by immunoblotting to verify the

localization of PsbQ and HopN1 in the thylakoid samples using the dilutions described above. Blots were also incubated with polyclonal anti-PsbA(D1) 1:5000 (AS05084 Agrisera); and anti-RbcL 1:4000 (Agrisera AS03 037-10), as thylakoid, and soluble fraction markers respectively. Samples were also incubated with monoclonal antibody MA1-6 (1:1000), which recognizes the *P. fluorescens* OprL protein (Hancock *et al.*, 1990).

In vitro *proteolysis analysis*

Thylakoid samples from *N. benthamiana* (25 μg of total protein) were incubated for 1 min at 30°C in lysis buffer (62.5 mM Tris-HCl pH 7.5; 2 mM $MgCl_2$) in the presence of soluble cell lysates (10 μg of total protein) of *E. coli* BL21 (DE3) carrying the pET-DEST42 plasmid (empty vector) or expressing the wild-type HopN1 protein (pCPP3390) or its non-catalytic HopN1D299A mutant version (pCPP3393). Samples were further subjected to SDS-PAGE [17.5% (w/v) gels] and analysed by immunoblotting using anti-PsbQ and anti-HopN1 antibodies. The immunoblot with the antibody directed against PsbA (thylakoid marker) was used to check for equal loading of the thylakoid protein samples.

Bacterial growth assays and symptom formation

Bacteria from frozen stocks were grown on plates for 2 days. A small amount of cells were resuspended in 100–200 μl liquid KB medium and spread on fresh plates and grown for 1 day. Cells were resuspended in 10 mM $MgCl_2$ and OD_{600} adjusted to 0.1 or 0.3, which is ~ $1–3 \times 10^8$ cfu ml^{-1}. Serial-fold dilutions were made in 10 mM $MgCl_2$ to achieve desired concentrations. The suspensions were plated in order to determine the actual cfu ml^{-1} used for inoculation.

Five-week-old *N. benthamiana* plants grown under greenhouse conditions with 2–3 well-expanded leaves were used for inoculation with bacteria prepared as described above, using a needle-less syringe. For growth assays, plants were then kept in a chamber at 24°C, 65% RH and constant light. At the desired time-point, three leaf discs (0.5 cm diameter) were excised from each spot and ground in 10 mM $MgCl_2$. Serial-fold dilutions were plated on KB agar with the relevant antibiotic, and bacteria counted after 2 days. Growth was expressed as log (cfu cm^{-2}). For the experiments involving symptom production with CUCPB5501, bacteria were adjusted to OD_{600} 0.1, diluted 10-fold, and up to three twofold dilutions were prepared and inoculated. The threshold inoculum level that showed a symptom difference between the samples (~ $0.3–0.5 \times 10^6$ cfu ml^{-1}) was used for comparisons in all replicate experiments. For experiments involving CUCPB6031, bacteria were adjusted to 10^5 cfu ml^{-1} and inoculated. At least six plants were inoculated in every experiment. To observe symptoms, plants were kept in a chamber at 24°C, 75% RH, and under fluorescent lights (Philips F32T8/TL841/XXL).

We thank C. Ramos and M. Barón for many fruitful discussions, and G. Salcedo and J. Murillo for reviewing the manuscript. We are very grateful to F. Sato and K. Ifuku for providing the *NtPsbQ*-silenced seeds. This research has been supported by the Spanish Plan Nacional I+D+I grants AGL2006-13503 and AGL-2009–12757. J.J.R.-H. is funded by the program 'Ramón y Cajal' from the Spanish Ministry of Science and Innovation (RYC-2007-01045). Z.L. was a recipient of a fellowship from the UPM-Bank Santander Sino-Spanish student exchange program. S. C. was supported by National Science Foundation Grant IOS-1025642.

Abbink, T.E., Peart, J.R., Mos, T.N., Baulcombe, D.C., Bol, J.F., and Linthorst, H.J. (2002) Silencing of a gene encoding a protein component of the oxygen-evolving complex of photosystem II enhances virus replication in plants. *Virology* **295:** 307–319.

Abramovitch, R.B., and Martin, G.B. (2004) Strategies used by bacterial pathogens to suppress plant defenses. *Curr Opin Plant Biol* **7:** 356–364.

Arnon, D.I. (1949) Copper enzymes in isolated chloroplasts. Polyphenoloxidase in *Beta Vulgaris*. *Plant Physiol* **24:** 1–15.

Aronsson, H., and Jarvis, P. (2002) A simple method for isolating import-competent *Arabidopsis* chloroplasts. *FEBS Lett* **529:** 215–220.

Boller, T., and Felix, G. (2009) A renaissance of elicitors: perception of microbe-associated molecular patterns and danger signals by pattern-recognition receptors. *Annu Rev Plant Biol* **60:** 379–406.

Bradley, D.J., Kjellbom, P., and Lamb, C.J. (1992) Elicitor- and wound-induced oxidative cross-linking of a proline-rich plant cell wall protein: a novel, rapid defense response. *Cell* **70:** 21–30.

Cascales, E., Bernadac, A., Gavioli, M., Lazzaroni, J.C., and Lloubès, R. (2002) Pal lipoprotein of *Escherichia coli* plays a major role in outer membrane integrity. *J Bacteriol* **184:** 754–759.

Chisholm, S.T., Coaker, G., Day, B., and Staskawicz, B.J. (2006) Host-microbe interactions: shaping the evolution of the plant immune response. *Cell* **124:** 803–814.

Coker, J., Vian, A., and Davies, E. (2005) Identification, accumulation, and functional prediction of novel tomato transcripts systemically upregulated after fire damage. *Physiol Plant* **124:** 311–322.

Cunnac, S., Lindeberg, M., and Collmer, A. (2009) *Pseudomonas syringae* type III secretion system effectors: repertoires in search of functions. *Curr Opin Microbiol* **12:** 53–60.

Cunnac, S., Chakravarthy, S., Kvitko, B.H., Russell, A.B., Martin, G.B., and Collmer, A. (2011) Genetic disassembly and combinatorial reassembly identify a minimal functional repertoire of type III effectors in *Pseudomonas syringae*. *Proc Natl Acad Sci USA* **108:** 2975–2980.

Doke, N. (1983) Involvement of superoxide anion generation in the hypersensitive response of potato tuber tissues to infection with an incompatible race of *Phytophthora infestans* and to the hyphal wall components. *Physiol Plant Pathol* **23:** 345–357.

Doke, N., and Ohashi, Y. (1988) Involvement of an O_2^--generating system in the induction of necrotic lesions on tobacco leaves infected with tobacco mosaic virus. *Physiol Mol Plant Pathol* **32:** 163–175.

Dowen, R.H., Engel, J.L., Shao, F., Ecker, J.R., and Dixon, J.E. (2009) A family of bacterial cysteine protease type III

effectors utilizes acylation-dependent and -independent strategies to localize to plasma membranes. *J Biol Chem* **284:** 15867–15879.

Felix, G., Duran, J.D., Volko, S., and Boller, T. (1999) Plants have a sensitive perception system for the most conserved domain of bacterial flagellin. *Plant J* **18:** 265–276.

Piñas-Fernández, A., and Strand, Å. (2008) Retrograde signaling and plant stress: plastid signals initiate cellular stress responses. *Curr Opin Plant Biol* **11:** 509–513.

Genoud, T., Buchala, A.J., Chua, N.H., and Métreaux, J.P. (2002) Phytochrome signaling modulates the SA-perspective pathway in *Arabidopsis*. *Plant J* **31:** 87–95.

Gohre, V., and Robatzek, S. (2008) Breaking the barriers: microbial effector molecules subvert plant immunity. *Annu Rev Phytopathol* **46:** 189–215.

Greenberg, J.T., and Yao, N. (2004) The role and regulation of programmed cell death in plant-pathogen interactions. *Cell Microbiol* **6:** 201–211.

Guo, M., Tian, F., Wamboldt, Y., and Alfano, J.R. (2009) The majority of the type III effector inventory of *Pseudomonas syringae* pv. tomato DC3000 can suppress plant immunity. *Mol Plant Microbe Interact* **22:** 1069–1080.

Hancock, R.E., Siehnel, R., and Martin, N. (1990) Outer membrane proteins of *Pseudomonas*. *Mol Microbiol* **4:** 1069–1075.

Huckelhoven, R. (2007) Cell wall-associated mechanisms of disease resistance and susceptibility. *Annu Rev Phytopathol* **45:** 101–127.

Ifuku, K., Yamamoto, Y., Ono, T.A., Ishihara, S., and Sato, F. (2005) PsbP protein, but not PsbQ protein, is essential for the regulation and stabilization of photosystem II in higher plants. *Plant Physiol* **139:** 1175–1184.

Ishiga, Y., Uppalapati, S.R., Ishiga, T., Elavarthi, S., Martin, B., and Bender, C.L. (2009a) Involvement of coronatine-inducible reactive oxygen species in bacterial speck disease of tomato. *Plant Signal Behav* **4:** 237–239.

Ishiga, Y., Uppalapati, S.R., Ishiga, T., Elavarthi, S., Martin, B., and Bender, C.L. (2009b) The phytotoxin coronatine induces light-dependent reactive oxygen species in 16 tomato seedlings. *New Phytol* **181:** 147–160.

Ishiga, Y., Ishiga, T., Wangdi, T., Mysore, K.S., and Uppalapati, S.R. (2011) NTRC and chloroplast-generated reactive oxygen species regulate *Pseudomonas syringae* pv. tomato disease development in tomato and *Arabidopsis*. DOI: 10.1094/*MPMI*-05-11-0130.

Jamir, Y., Guo, M., Oh, H.S., Petnicki-Ocwieja, T., Chen, S., Tang, X., *et al.* (2004) Identification of *Pseudomonas syringae* type III effectors that can suppress programmed cell death in plants and yeast. *Plant J* **37:** 554–565.

Jelenska, J., Yao, N., Vinatzer, B.A., Wright, C.M., Brodsky, J.L., and Greenberg, J.T. (2007) A J domain virulence effector of *Pseudomonas syringae* remodels host chloroplasts and suppresses defenses. *Curr Biol* **17:** 499–508.

Jones, A.M., Thomas, V., Bennett, M.H., Mansfield, J., and Grant, M. (2006) Modifications to the *Arabidopsis* defense proteome occur prior to significant transcriptional change in response to inoculation with *Pseudomonas syringae*. *Plant Physiol* **142:** 1603–1620.

Jones, J.D., and Dangl, J.L. (2006) The plant immune system. *Nature* **444:** 323–329.

Kaku, H., Nishizawa, Y., Ishii-Minami, N., Akimoto-Tomiyama, C., Dohmae, N., Takio, K., *et al.* (2006) Plant cells recognize chitin fragments for defense signaling through a plasma membrane receptor. *Proc Natl Acad Sci USA* **103:** 11086–11091.

King, E.O., Ward, M.K., and Raney, D.E. (1954) Two simple media for the demonstration of pyocyanin and fluorescin. *J Lab Clin Med* **44:** 301–307.

Krause, M., and Durner, J. (2004) Harpin inactivates mitochondria in *Arabidopsis* suspension cells. *Mol Plant Microbe Interact* **17:** 131–139.

Kvitko, B.H., Park, D.H., Velásquez, A.C., Wei, C.-F., Russell, A.B., Martin, G.B., *et al.* (2009) Deletions in the repertoire of *Pseudomonas syringae* pv. *tomato* DC3000 type III secretion effector genes reveal functional overlap among effectors. *PLoS Pathog* **5:** e1000388.

Lamb, C.J., Ryals, J.A., Ward, E.R., and Dixon, R.A. (1992) Emerging strategies for enhancing crop resistance to microbial pathogens. *Biotechnology (N Y)* **10:** 1436–1445.

Levine, A., Tenhaken, R., Dixon, R., and Lamb, C. (1994) H_2O_2 from the oxidative burst orchestrates the plant hypersensitive disease resistance response. *Cell* **79:** 583–593.

Lin, N.C., Abramovitch, R.B., Kim, Y.J., and Martin, G.B. (2006) Diverse AvrPtoB homologs from several *Pseudomonas syringae* pathovars elicit Pto-dependent resistance and have similar virulence activities. *Appl Environ Microbiol* **72:** 702–712.

Liu, Y., Ren, D., Pike, S., Pallardy, S., Gassmann, W., and Zhang, S. (2007) Chloroplast-generated reactive oxygen species are involved in hypersensitive response-like cell death mediated by a mitogen-activated protein kinase cascade. *Plant J* **51:** 941–954.

López-Solanilla, E., Bronstein, P.A., Schneider, A.R., and Collmer, A. (2004) HopPtoN is a *Pseudomonas syringae* Hrp (type III secretion system) cysteine protease effector that suppresses pathogen-induced necrosis associated with both compatible and incompatible plant interactions. *Mol Microbiol* **54:** 353–365.

Mur, L.A., Kenton, P., Lloyd, A.J., Ougham, H., and Prats, E. (2008) The hypersensitive response; the centenary is upon us but how much do we know? *J Exp Bot* **59:** 501–520.

Naidu, R., Krishnan, M., Nayudu, M., and Gnanam, A. (1986) Studies on peanut green mosaic virus infected peanut (*Arachis hypogaea* L.) leaves. III. Changes in the polypeptides of photosystem II particles. *Physiol Mol Plant Pathol* **29:** 53–58.

Navarro, L., Jay, F., Nomura, K., He, S.Y., and Voinnet, O. (2008) Suppression of the microRNA pathway by bacterial effector proteins. *Science* **321:** 964–967.

Oh, H.S., Park, D.H., and Collmer, A. (2010) Components of the *Pseudomonas syringae* type III secretion system can suppress and may elicit plant innate immunity. *Mol Plant Microbe Interact* **23:** 727–739.

Padmanabhan, M.S., and Dinesh-Kumar, S.P. (2010) All hands on deck-the role of chloroplasts, endoplasmic reticulum, and the nucleus in driving plant innate immunity. *Mol Plant Microbe Interact* **23:** 1368–1380.

Pérez-Bueno, M.L., Rahoutei, J., Sajnani, C., Garcia-Luque, I., and Baron, M. (2004) Proteomic analysis of the oxygen-evolving complex of photosystem II under biotec stress: studies on *Nicotiana benthamiana* infected with tobamoviruses. *Proteomics* **4:** 418–425.

Piedras, P., Hammond-Kosack, K.E., Harrison, K., and Jones, J.D.G. (1998) Rapid, Cf-9- and Avr9-dependent production of active oxygen species in tobacco suspension cultures. *Mol Plant Microbe Interact* **11:** 1155–1166.

del Pozo, O., Pedley, K.F., and Martin, G.B. (2004) MAPKKKalpha is a positive regulator of cell death associated with both plant immunity and disease. *EMBO J* **23:** 3072–3082.

Roose, J.L., Wegener, K.M., and Pakrasi, H.B. (2007) The extrinsic proteins of Photosystem II. *Photosynth Res* **92:** 369–387.

Shao, F., Merritt, P.M., Bao, Z., Innes, R.W., and Dixon, J.E. (2002) A *Yersinia* effector and a *Pseudomonas* avirulence protein define a family of cysteine proteases functioning in bacterial pathogenesis. *Cell* **109:** 575–588.

Takahashi, H., and Ehara, Y. (1992) Changes in the activity and the polypeptide composition of the oxygen-evolving complex in photosystem II of tobacco leaves infected with cucumber mosaic virus strain Y. *Mol Plant Microbe Interact* **5:** 269–272.

Takahashi, H., Ehara, Y., and Hirano, H. (1991) A protein in the oxygen-evolving complex in the chloroplast is associated with symptom expression on tobacco leaves infected with cucumber mosaic virus strain Y. *Plant Mol Biol* **16:** 689–698.

Tao, Y., Xie, Z., Chen, W., Glazebrook, J., Chang, H.S., Han, B., *et al.* (2003) Quantitative nature of *Arabidopsis* responses during compatible and incompatible interactions with the bacterial pathogen *Pseudomonas syringae*. *Plant Cell* **15:** 317–330.

Thordal-Christensen, H., Zhang, Z., Wei, Y., and Collinge, D. (1997) Subcellular localization of H_2O_2 in plants. H_2O_2 accumulation in papillae and hypersensitive response during the barley-powdery mildew interaction. *Plant J* **11:** 1187–1194.

de Torres, M., Mansfield, J.W., Grabov, N., Brown, I.R., Ammouneh, H., Tsiamis, G., *et al.* (2006) *Pseudomonas syringae* effector AvrPtoB suppresses basal defence in *Arabidopsis*. *Plant J* **47:** 368–382.

Torres, M.A., and Dangl, J.L. (2005) Functions of the respiratory burst oxidase in biotic interactions, abiotic stress and development. *Curr Opin Plant Biol* **8:** 397–403.

Torres, M.A., Dangl, J.L., and Jones, J.D. (2002) *Arabidopsis* gp91^{phox} homologues *AtrbohD* and *AtrbohF* are required for accumulation of reactive oxygen intermediates in the plant defense response. *Proc Natl Acad Sci USA* **99:** 517–522.

Tsuda, K., and Katagiri, F. (2010) Comparing signaling mechanisms engaged in pattern-triggered and effector-triggered immunity. *Curr Opin Plant Biol* **13:** 459–465.

Wei, C.F., Kvitko, B.H., Shimizu, R., Crabill, E., Alfano, J.R., Lin, N.C., *et al.* (2007) A *Pseudomonas syringae* pv. *tomato* DC3000 mutant lacking the type III effector HopQ1-1 is able to cause disease in the model plant *Nicotiana benthamiana*. *Plant J* **51:** 32–46.

Weigel, D., and Glazebrook, J. (2002) How to transform *Arabidopsis*. In *Arabidopsis: A Laboratory Manual*. Weigel, D., and Glazebrook, J. (eds). Cold Spring Harbor, NY, USA: Cold Spring Harbor Laboratory Press, pp. 119–140.

Yi, X., Hargett, S.R., Frankel, L.K., and Bricker, T.M. (2006) The PsbQ protein is required in *Arabidopsis* for photosystem II assembly/stability and photoautotrophy under low light conditions. *J Biol Chem* **281:** 26260–26267.

Zeier, J., Pink, B., Mueller, M.J., and Berger, S. (2004) Light conditions influence specific defence responses in incompatible plant-pathogen interactions: uncoupling systemic resistance from salicylic acid and PR-1 accumulation. *Planta* **219:** 673–683.

Zurbriggen, M.D., Carrillo, N., Tognetti, V.B., Melzer, M., Peisker, M., Hause, B., and Hajirezaei, M.R. (2009) Chloroplast-generated reactive oxygen species play a major role in localized cell death during the non-host interaction between tobacco and *Xanthomonas campestris* pv. *vesicatoria*. *Plant J* **60:** 962–973.

Additional Supporting Information may be found in the online version of this article:

Fig. S1. DAB staining and callose deposition in tomato leaves.
Fig. S2. Identification of HopN1 target by liquid chromatography and MS analysis.
Fig. S3. Subcellular localization of HopN1 protein in onion epidermal cells.
Fig. S4. Confirmation of the phenotype of the *NtPsbQ*-silenced tobacco plants.
Table S1. Data from the quantification of the DAB signal and aniline blue fluorescence corresponding to the histograms shown in Fig. 1 (*Arabidopsis* leaves) and Fig. S1 (tomato leaves).
Table S2. PSII activity in isolated tomato chloroplasts.
Table S3. Quantification of the DAB signal on snapshots from infected leaves of WT and *NtPsbQ*-silenced tobacco plants.
Table S4. Bacterial strains and plasmids.